Immunoproteasomes largely replace constitutive proteasomes during an antiviral and antibacterial immune response in the liver

Khan, S ; van den Broek, M ; Schwarz, K ; de Giuli, R ; Diener, P A ; Groettrup, M

Abstract: The proteasome is critically involved in the production of MHC class I-restricted T cell epitopes. Proteasome activity and epitope production are altered by IFN-gamma treatment, which leads to a gradual replacement of constitutive proteasomes by immunoproteasomes in vitro. However, a quantitative analysis of changes in the steady state subunit composition of proteasomes during an immune response against viruses or bacteria in vivo has not been reported. Here we show that the infection of mice with lymphocytic choriomeningitis virus or Listeria monocytogenes leads to an almost complete replacement of constitutive proteasomes by immunoproteasomes in the liver within 7 days. Proteasome replacements were markedly reduced in IFN-gamma(-/-) mice, but were only slightly affected in IFN-alphaR(-/-) and perforin(-/-) mice. The proteasome regulator PA28alpha/beta was up-regulated, whereas PA28gamma was reduced in the liver of lymphocytic choriomeningitis virus-infected mice. Proteasome replacements in the liver strongly altered proteasome activity and were unexpected to this extent, since an in vivo half-life of 12 days had been previously assigned to constitutive proteasomes in the liver. Our results suggest that during the peak phase of viral and bacterial elimination the antiviral cytotoxic T lymphocyte response is directed mainly to immunoproteasome-dependent T cell epitopes, which would be a novel parameter for the design of vaccines.

DOI: https://doi.org/10.4049/jimmunol.167.12.6859

Immunoproteasomes Largely Replace Constitutive Proteasomes During an Antiviral and Antibacterial Immune Response in the Liver[1]

Selina Khan,[2]* Maries van den Broek,[2‡] Katrin Schwarz,[2]* Rita de Giuli,* Pierre-André Diener,[†] and Marcus Groettrup[3]*

The proteasome is critically involved in the production of MHC class I-restricted T cell epitopes. Proteasome activity and epitope production are altered by IFN-γ treatment, which leads to a gradual replacement of constitutive proteasomes by immunoproteasomes in vitro. However, a quantitative analysis of changes in the steady state subunit composition of proteasomes during an immune response against viruses or bacteria in vivo has not been reported. Here we show that the infection of mice with lymphocytic choriomeningitis virus or *Listeria monocytogenes* leads to an almost complete replacement of constitutive proteasomes by immunoproteasomes in the liver within 7 days. Proteasome replacements were markedly reduced in IFN-$\gamma^{-/-}$ mice, but were only slightly affected in IFN-αR$^{-/-}$ and perforin$^{-/-}$ mice. The proteasome regulator PA28α/β was up-regulated, whereas PA28γ was reduced in the liver of lymphocytic choriomeningitis virus-infected mice. Proteasome replacements in the liver strongly altered proteasome activity and were unexpected to this extent, since an in vivo half-life of 12 days had been previously assigned to constitutive proteasomes in the liver. Our results suggest that during the peak phase of viral and bacterial elimination the antiviral cytotoxic T lymphocyte response is directed mainly to immunoproteasome-dependent T cell epitopes, which would be a novel parameter for the design of vaccines. *The Journal of Immunology,* **2001, 167: 6859–6868.**

The proteasome is a proteolytic system that selectively terminates the function of proteins in the cell by degrading them to peptides (1). The immune system makes use of these peptides as ligands for MHC class I molecules to be presented to CTL. As part of the MHC class I pathway the immune system has developed the ability to modify proteasome activity in inflammatory sites through the cytokine-mediated induction and replacement of proteasome active site subunits and regulators (2). Although this phenomenon has been studied extensively in vitro, little is known about the extent to which proteasome subunit replacements occur during an ongoing immune response in an inflamed tissue in vivo. Hence, we decided to examine the subunit composition of proteasomes in the liver of lymphocytic choriomeningitis virus (LCMV)-[4] and *Listeria monocytogenes* (Lm)-infected mice.

The proteasome system consists of a proteolytic core unit, the 20S proteasome, and regulators such as PA700, PA28α/β, PA28γ, and PI31, which control substrate acquisition and catalytic activity of the proteasome. The 20S proteasome is constructed like a barrel of four stacked rings. The two outer rings contain seven different subunits of the α type, whereas the inner two rings contain seven different subunits of the β type that are numbered according to their positions in the ring. The subunits β1 (δ,Y), β2 (MC14, LMP9, Z), and β5 (MB1, X) bear the catalytically active sites of the 20S proteasome facing the inner cavity of the protease. When cells are treated with the inflammatory cytokines IFN-γ and TNF-α, three additional active site subunits, named β1i (LMP2), β2i (MECL-1), and β5i (LMP7), are transcriptionally induced and take the place of their constitutive homologues during proteasome neosynthesis. This substitution of active site subunits changes the proteolytic specificity of the proteasome (3–6) and leads to marked changes in the distribution of fragments that are produced from polypeptides (7, 8). The exchange of LMP2 for δ was unanimously reported to down-regulate cleavages C-terminal of acidic residues (the caspase-like activity) and favor the cleavage C-terminal of hydrophobic residues (the chymotrypsin-like activity). This change in cleavage specificity conforms to structural requirements of class I peptide ligands that possess hydrophobic C termini in the mouse and either hydrophobic or basic C termini in the human. Conflicting data have been reported on the effects of the two other subunit exchanges of LMP7 for MB1 (8–10) and MECL-1 for MC14 (Z) (11), and structural analysis does not predict major changes in the specificity of the P1 pockets (12), leaving the functions of these latter two exchanges elusive. With respect to the bulk production of MHC class I ligands, it was found in LMP2- and LMP7-deficient cell lines (13, 14) that these subunits are not generally required to maintain class I cell surface expression. For the generation of specific epitopes, however, the expression of either LMP2 or LMP7 can be pivotal. Several epitopes were produced

*Research Department and [†]Institute for Pathology, Cantonal Hospital St. Gallen, St. Gallen, Switzerland; and [‡]Institute of Experimental Immunology, Department of Pathology, University Hospital Zurich, Zurich, Switzerland

Received for publication April 3, 2001. Accepted for publication October 17, 2001.

The costs of publication of this article were defrayed in part by the payment of page charges. This article must therefore be hereby marked *advertisement* in accordance with 18 U.S.C. Section 1734 solely to indicate this fact.

[1] This work was supported by grants from the Swiss National Science Foundation (31-52284.97/1), the Roche Research Foundation, the Novartis Foundation, and the Rentenanstalt Jubiläumsstiftung (to M.G.) and by a grant from the Cloëtta Foundation (to M.v.d.B.).

[2] S.K., M.v.d.B., and K.S. contributed equally to this work and are all considered first authors.

[3] Address correspondence and reprint requests to Dr. Marcus Groettrup, Kantonsspital St. Gallen, LFA, Haus 09, CH-9007 St. Gallen, Switzerland. E-mail address: marcus.groettrup@kssg.ch

[4] Abbreviations used in this paper: LCMV, lymphocytic choriomeningitis virus; a.t., annealing temperature; ER, endoplasmic reticulum; HPRT, hypoxanthine phosphoribosyltransferase; Lm, *Listeria monocytogenes*; NEPHGE, nonequilibrium pH gradient gel electrophoresis; βNA, β-nitroanilide; MCA, 7-amido-4-methylcoumarin; moLMP, mouse LMP.

0022-1767/01/$02.00

inefficiently or not at all in the absence of LMP2 (15, 16) or LMP7 (17–22), but the opposite case has recently been reported for several epitopes from tumor Ags that were destroyed when LMP2 and LMP7 were expressed at high levels (23). Consistent with these in vitro results, it was recently found in LMP2$^{-/-}$ mice that this subunit has a pivotal influence on the hierarchy of T cell epitopes from influenza virus (24).

A further component of the proteasome system that has a pronounced effect on Ag processing is the proteasome regulator PA28α/β. Both, the α and β subunits of this ring-shaped regulator are inducible with IFN-γ at both mRNA and protein levels (25). PA28α/β stimulates the various proteolytic activities of the proteasome to different extents and markedly alters the fragmentation of polypeptides through the 20S proteasome (8, 26, 27). Overexpression of PA28α/β in cell lines resulted in a higher presentation of some (28–30), but not all, T cell epitopes (22), suggesting a role for PA28α/β in Ag processing that was recently confirmed in PA28$\beta^{-/-}$ mice (31). A homologue of PA28α/β that is not transcriptionally induced by IFN-γ is named Ki Ag or PA28γ. The single subunit of PA28γ forms heptahomomeric rings that associate with the proteasome and are predominantly found in the nucleus. Interestingly, the PA28γ protein appears to be down-regulated upon the IFN-γ treatment of cell lines in vitro and in transgenic mice that constitutively express IFN-γ in the liver (32). PA28$\gamma^{-/-}$ mice were slightly retarded in growth (33), but the function of PA28γ that causes this phenotype has remained elusive.

Taken together it appears that the inducible proteasome subunits LMP2, LMP7, and MECL-1 as well as the proteasome regulator PA28α/β are not needed to guarantee the bulk flow of MHC class I ligands, but for the generation of unique epitopes they often have a decisive impact. Based on these insights, two hypotheses can be envisaged as to why the immunoproteasomes and PA28α/β coevolved with the MHC class I pathway. It may be that these factors are induced to generate different sets of proteasome complexes in a cell to enlarge the diversity of peptide processing, which would allow the processing of a given antigenic protein in several ways. For this scenario it should be useful to express approximately equal amounts of constitutive proteasomes and immunoproteasomes in an inflamed tissue. Alternatively, it could be that CTLs are meant to be directed to a different set of peptides in an inflammatory site compared with noninflamed tissues, and this could only be achieved if constitutive proteasomes were largely replaced by immunoproteasomes. We have investigated in this study the steady state composition of 20S proteasomes of the liver on several days during the course of an infection of the mouse with the hepatotropic WE strain of LCMV and the bacterium Lm. Unexpectedly, the infections led to virtually complete replacement of constitutive proteasomes by immunoproteasomes and strong induction of PA28α/β as well as the disappearance of PA28γ on days 7 and 8 of the infection, when the cytotoxic immune response is maximal and pathogen numbers decline. Our results suggest that the cytotoxic immune response in the infected liver will be predominantly directed to a set of T cell epitopes that are produced by immunoproteasomes, while the T cell response is clearing the virus. This finding argues against the maximal diversity argument and suggests that it must be beneficial for the immune response to convert epitope production to a set of peptides that is produced by immunoproteasomes and PA28α/β.

Materials and Methods

Mice and cell lines

C57BL/6 mice (H-2^b) and BALB/c mice (H-2^d) were purchased from Institut für Labortierkunde, Tierspital Zurich (Zurich, Switzerland), and kept in a specific pathogen-free environment. Mice deficient for IFN-γ (34), IFN-αR (35), and perforin (36) have been described previously. MC57 is a C57BL/6-derived methylcholantrene-induced fibrosarcoma cell line (37), and B8 is a BALB/c-derived SV40-induced fibroblast line (38). H2.35 is a mouse hepatocyte cell line that we obtained from American Type Culture Collection (Manassas, VA). All cell lines were grown in IMDM or RPMI 1640 medium supplemented 10% FCS, 2 mM L-glutamine, and 100 U/ml penicillin/streptomycin.

Flow cytometry

For surface staining, aliquots of 5×10^5 cells in PBS and 2% FCS were incubated for 15 min in a round-bottom 96-well plate on ice with the mouse mAb KL25 specific for the LCMV glycoprotein (39). The cells were washed three times and subsequently stained by FITC-conjugated goat anti-mouse Ig secondary Ab (Silenus, Melbourne, Australia). After two washing steps the cells were analyzed on a FACScan flow cytometer (BD Biosciences, Mountain View, CA).

LCMV, Listeria*, and infection of mice*

LCMV-WE was propagated in the L929 fibroblast line, and viral stocks were kept at −70°C (40). The virus was grown and titrated on L929 cells exactly as previously described (41). Mice were infected i.v. with 200 PFU (low dose) or 10^6 PFU (high dose) LCMV-WE. After the indicated days the mice were sacrificed, and the livers were excised for purification of 20S proteasomes and for Western analysis. Spleen and liver samples were used for determination of LCMV titers, and peripheral blood was used for IFN-γ ELISA. Serum levels of IFN-γ were below detection levels on all days of infection except day 4, when 10–30 U/ml was found.

For *Listeria* infection, mice were infected i.v. with 9800 CFU Lm 10304S in PBS. Lm were cultured overnight at 37°C in brain-heart infusion broth. On the day of infection, 10-fold serial dilutions of the inoculum were plated on brain-heart infusion agar plates and incubated overnight at 37°C. The exact amount of bacteria injected the day before was calculated from these plates.

Purification of 20S proteasomes from mouse liver and fluorogenic assays

20S proteasomes from two or three mouse livers were purified and quantitated as detailed previously (42). Hydrolytic assays for proteasome activity employing fluorogenic assays were performed as previously described (43). PA28α/β complexes were not detected in the proteasome preparations according to Western analysis (data not shown).

Two-dimensional gel electrophoresis

For Figs. 2–5 aliquots of 60 μg purified 20S proteasomes were separated on two-dimensional nonequilibrium pH gradient gel electrophoresis (NEPHGE)/SDS-PAGE or isoelectric focusing/SDS-PAGE exactly as previously described (44). After the run, the gels were stained with Coomassie brilliant blue R250. For quantitation, the gels were scanned and analyzed using AIDA software (Fuji, Tokyo, Japan).

Metabolic labeling and immunoprecipitation

H2.35, B8, or MC57 cells were left untreated or were infected with LCMV-WE at a multiplicity of infection of 0.01. One day after infection cells were incubated with 100 U/ml mouse rIFN-γ for 16 h or were left unstimulated. LCMV infection was confirmed flow cytometrically by LCMV glycoprotein expression on the cell surface, and IFN-γ stimulation was confirmed by up-regulation of H-2 class I expression. Cells were starved in methionine/cysteine-free RPMI 1640 and 10% dialyzed FCS with or without rIFN-γ for 30 min, labeled for 6 h with 0.2 mCi/ml Trans ^{35}S label (ICN, Eschwege, Germany), and chased for 18 h with or without rIFN-γ. The cells were harvested by trypsinization and lysed by sonication in buffer A (25 mM Tris (pH 7.6), 2 mM $MgCl_2$, 17% glycerol, 1 mM DTT, and 2 mM ATP). The postnuclear lysates were counted for ^{35}S incorporation, and equal aliquots were used for immunoprecipitation. The lysate was precleared for 1 h with protein G-Sepharose CL-4B (Pharmacia, Uppsala, Sweden), followed by immunoprecipitation with an anti-proteasome serum (30) bound to protein G-Sepharose for 4 h at 4°C. The precipitates were washed with buffer A, separated by NEPHGE/SDS-PAGE, and visualized on x-ray films by autoradiography.

Western blot analysis and sucrose gradient density centrifugation

In Fig. 6 liver specimens were lysed in buffer B (50 mM Tris-HCl (pH 7.5), 5 mM $MgCl_2$, 1 mM EDTA, 1% SDS, 0.75 μM aprotinin, 10 μM leupeptin, 2.8 μM pepstatin, and 0.85 mM PMSF) in a Dounce homogenizer (Kontes, Vineland, NJ), and 100 μg total protein/lane was separated by SDS-PAGE. In Fig. 2*D* liver samples from C57BL6 mice on day 8 of LCMV infection were lysed in buffer C (25 mM Tris-HCl (pH 7.5) and 2 mM $MgCl_2$) in a Dounce homogenizer with subsequent sonication. Postnuclear supernatants were loaded onto a 10–40% sucrose gradient and centrifuged at 40,000 rpm in a Beckman SW40Ti rotor (Palo Alto, CA) for 16 h. Gradient fractions of 0.6 ml were drawn, proteasome activity was determined to confirm proper separation, and proteins were separated on SDS-PAGE. The proteins were blotted onto nitrocellulose membrane (Schleicher & Schuell, Dassel, Germany), blocked with PBS/5% (w/v) low fat dry milk/0.1% Tween 20 for 1 h, and agitated overnight at 4°C with the described rabbit antisera specific for peptides PA28α and PA28β (45). Rabbit antisera for mouse LMP7 and PA28γ were raised against the keyhole limpet hemocyanin-coupled peptides SDVSDLLYKYGEAAL and ILLTNSHDGLDGPTYK, respectively. The MC3 Ab has been described previously (46). The blots were washed and incubated for 1 h with HRP-conjugated secondary Ab. After extensive washing with PBS/0.1% Tween 20, proteins were visualized on x-ray films by enhanced chemiluminescence.

Real-time RT-PCR

Total RNA was extracted from mouse liver tissue using TRIzol reagent (Life Technologies, Basel, Switzerland). cDNA was synthesized from 3 μg RNA using 2 mM dT15, 2 mM dNTPs, 0.6 U/μl RNasin (Promega, Wallisellen, Switzerland), 200 U Moloney murine leukemia virus RT (Promega)/reaction (1 h at 42°C). After cDNA synthesis, the nucleic acids were precipitated in 0.3 M NaCl/80% ethanol, and the pellet was washed twice in 70% ethanol. The samples were resuspended in H_2O. Real-time PCR was performed with a Light Cycler (Roche, Basel) using the DNA Master SYBR Green I reaction mix (Roche) and 0.5 pmol/μl of each primer in 3.5 mM $MgCl_2$. Sense and antisense primers used for PCR amplification were (annealing temperatures (a.t.) given in parentheses): mouse (mo) LMP2, 5′-TCCACACCGGGACAACC-3′ and 5′-CCAGCCAGCTACTATGAG ATGC-3′ (a.t. = 62°C); moDELTA, 5′-TCGAGTGACTGACAAGCT GACC-3′ and 5′-GAACAGAGTACACCTGCCCTCC-3′ (a.t. = 62°C); moLMP7, 5′-CTCCGTGTCTGCAGCATCC-3′ and 5′-TCCACTTTCAC CCAACCGTC-3′ (a.t. = 58°C); moMB1, 5′-CTTGACGGAACCACCACC-3′ and 5′-CCATAGACAGCCCCATGC-3′ (a.t. = 58°C); moTNF-α, 5′-GCACA GAAAGCATGATCC-3′ and 5′-TGTCCCTTGAAGAGAACC-3′ (a.t. = 62°C); and mouse hypoxanthine phosphoribosyltransferase (HPRT): 5′-GCTGGTGAAAAGGACCTC-3′ and 5′-CACAGGACTAGAACACCTGC-3′ (a.t. = 60°C). The runs were programmed as follows: denaturation for 30 s at 95°C; amplification (40 cycles, with readings of the fluorescence at the end of each cycle) for 1 s at 95°C, 10 s at a.t., and 20 s at 72°C; and analysis of the products (reading of the fluorescence in a continuous mode) for 0 s at 95°C, 62 to 95°C transition with 0.1°C increment/sec. For mouse IFN-γ we used a conventional PCR mix containing the PCR primers moIFNγ (5′-GACAATGAACGCTACACACTGC-3′ and 5′-GGACAATCTCTTC CCCACC-3′; a.t. = 58°C) and the fluorescence resonance energy transfer primers (5′-TGCCAAGTTTGAGGTCAACAACCCACA-fluorescein-3′ and 5′-LCred640-GTCCAGCGCCAAGCATTCAATGAGC-3′); reading of fluorescence was performed after annealing. Analysis was performed with Light Cycler software 3. The value calculated by the quantification analysis was always within the range covered by three concentrations of sample that were taken as arbitrary units to construct the standard curve for linear regression with $r = 1.0$ and $p < 0.0001$. The cDNAs were normalized to HPRT mRNA content. The specificity of the amplification was checked with melting curve analysis of the products as well as analysis on an agarose gel.

Results

LCMV-WE does not induce immunoproteasomes by itself and does not interfere with the IFN-γ-mediated induction of immunoproteasomes

To investigate how the steady state composition of 20S proteasome subunits changes during the course of a viral infection it was important to choose a virus that infects an entire organ in a well-documented manner and reproducible time course. The infection of the mouse with the hepatotropic strain WE of LCMV is a suitable model system to address this question, because this virus readily replicates in hepatocytes, Kupffer cells, fibroblasts, endothelial cells, and other cell types of the liver, and it rapidly spreads throughout the organ (47–49). Moreover, LCMV-WE elicits a strong and well-characterized CTL response that is maximal on day 8 of infection and leads to elimination of the virus. However, as some viruses interfere with the induction of immunoproteasomes (50, 51), we decided to initially test whether this was also the case for LCMV-WE. The mouse hepatocyte line H2.35 as well as B8 or MC57 fibroblasts were infected with LCMV-WE and after 1 day were cultivated in the presence or the absence of IFN-γ for 16 h before metabolic labeling. Proteasomes were immunoprecipitated, and the subunit composition was analyzed by two-dimensional NEPHGE/SDS-PAGE (Fig. 1*A*). Inductions of LMP2 or LMP7 were not observed in H2.35 cells (Fig. 1) or in B8 or MC57 cells (data not shown) upon LCMV-WE infection, although the cells were productively infected, as documented by flow cytometric analysis of LCMV glycoprotein expression on the cell surface (data not shown). Moreover, an interference of LCMV-WE with the IFN-γ mediated induction of LMP2 and LMP7 was not observed, which was a prerequisite for monitoring their in vivo induction in infected mice.

Gradual and extensive replacement of constitutive proteasomes by immunoproteasomes in the liver of LCMV-infected mice

Mice of the C57BL/6 strain were infected i.v. with a high dose (10^6 PFU) of LCMV-WE, and two livers each from uninfected mice and mice on days 2, 4, 8, 12, and 25 after infection were used to purify 20S proteasomes. The subunits of the 20S proteasomes were separated by two-dimensional NEPHGE/SDS-PAGE, and the proteins were visualized by Coomassie staining. This method allows a reliable quantification of the steady state amounts of proteasome subunits and the relative intensity changes during subunit replacements. The results shown in Fig. 2*A* reveal that uninfected mice express very little LMP2 and LMP7 in the liver compared with the constitutive subunits δ and MB1. The protein spots for these four subunits as well as the constitutive and invariant α-type subunit C6 were quantified by densitometry, and the data are shown in Fig. 2*B*. On day 2 postinfection the inducible subunits had already begun to rise, and by day 4 LMP2 and δ were equally

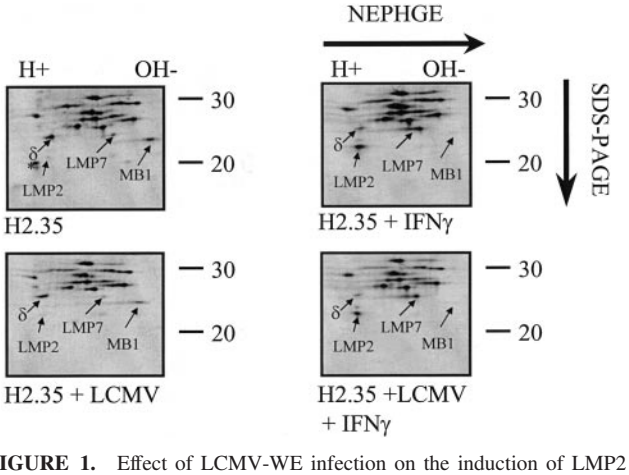

FIGURE 1. Effect of LCMV-WE infection on the induction of LMP2 and LMP7. *A*, NEPHGE/SDS-PAGE of proteasome immunoprecipitates from metabolically labeled H2.35 hepatocytes. Cells were treated for 2 days with rIFN-γ and/or infected with LCMV-WE as indicated below each autoradiography. The positions of the proteasome subunits LMP2 (β1i), LMP7 (β5i), Δ (β1), and MB1 (β5) are marked by arrows; the molecular mass is given in kilodaltons at the *right*. The spot marked with an asterisk in the *top left panel* is unspecific.

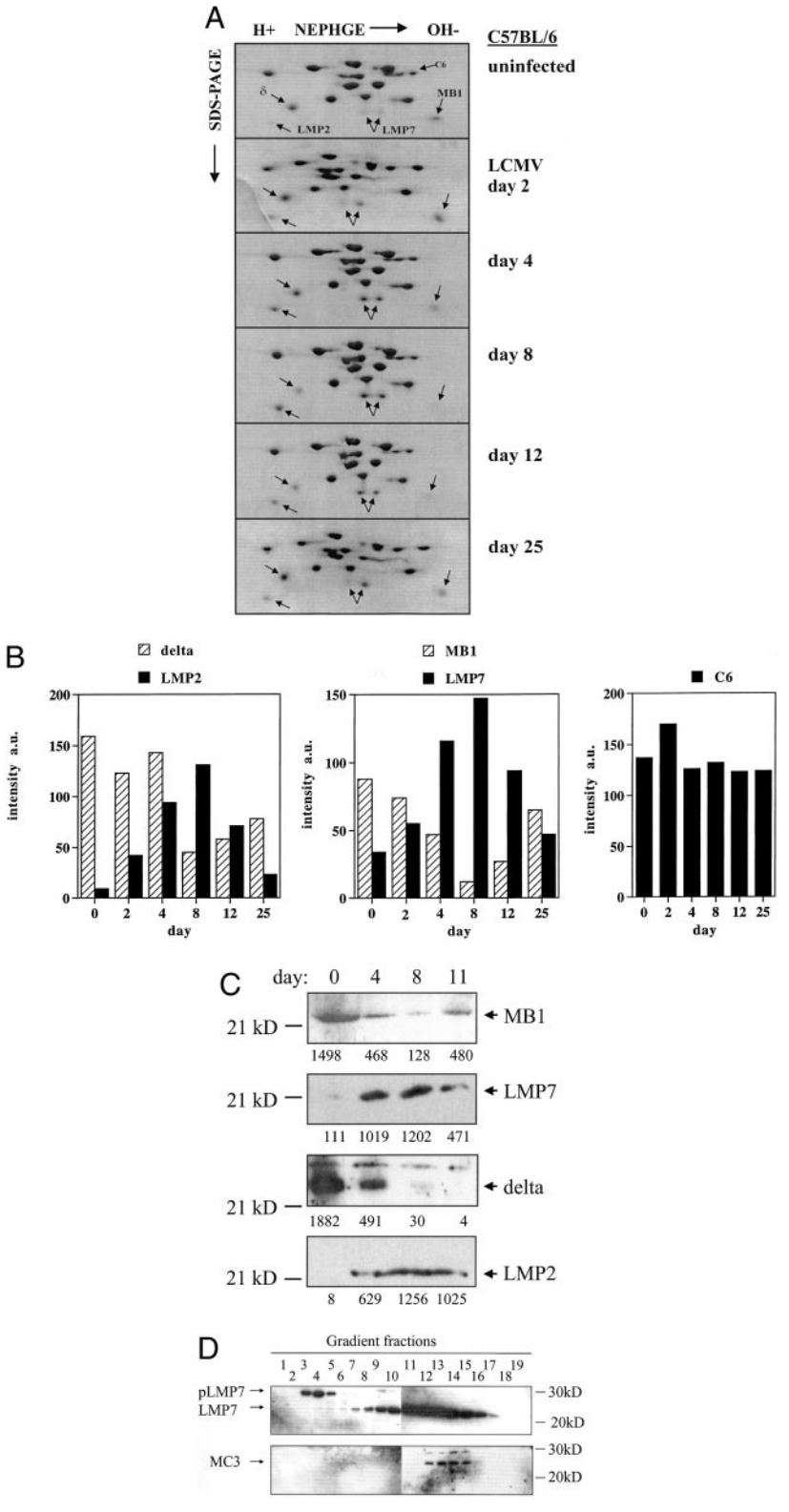

FIGURE 2. Composition of 20S proteasome subunits purified from livers of LCMV-WE-infected C57BL/6 mice. *A*, NEPHGE/SDS-PAGE analysis of 60 μg 20S proteasome purified from the liver of uninfected mice or mice that had been infected with a high dose of LCMV-WE (10^6 PFU) on the indicated days before organ removal. The proteins were visualized by Coomassie stain. The positions of proteasome subunits LMP2, LMP7, Δ, MB1, and C6 are indicated; the two spots assigned to LMP7 were confirmed by Western blotting (not shown). *B*, Densitometric evaluation of indicated proteasome subunits from the two-dimensional gels shown in *A*. *C*, Western analysis of the proteasome subunits MB1, LMP7, δ, and LMP2 in livers of LCMV-WE-infected C57BL/6 mice. The day of infection is indicated at the *top*, and the results of densitometric analysis of bands on x-ray films are shown below each lane in arbitrary units (a.u.). *D*, LMP7 and MC3 Western analysis of sucrose gradient fractions prepared from livers of C57BL/6 mice on day 8 after LCMV infection. Proteasome activity was detected in fractions 12–14. Note the presence of monomeric LMP7 precursors (pLMP7) at the *top* of the gradient.

prominent, whereas the LMP7 spots were already twice as intensive as that for MB1. On day 8 of infection, when virus titers start to decline (Table I) and the cytotoxic immune response and the expansion of LCMV-specific $CD8^+$ T cells are usually maximal (47, 52), we observed an almost complete replacement of δ by LMP2 and of MB1 by LMP7. The 8-fold reduction of MB1 and the 4-fold reduction of δ by day 8 of infection were unexpected, as the constitutive proteasome was reported to possess an in vivo half-life of 12–15 days in rat livers (53). The exchange of MC14 by MECL-1 on day 8 was analyzed on isoelectric focusing-SDS-PAGE two-dimensional gels, because it was not readily resolved by NEPHGE/SDS-PAGE and was found to occur to an extent of only 50% (data not shown) as has been previously documented for IFN-γ-treated cells (44). On day 12 postinfection, when virus titers were 100-fold reduced, the ratio of inducible to constitutive subunits started to revert again, but even on day 25 of infection the

Table I. *LCMV titers in liver samples from mice at indicated days after infection with high (10^6 PFU) or low (200 PFU) doses of LCMV-WE*[a]

Mouse Strain	Dose of Infection	Day of Infection	LCMV Titer
C57BL/6	High	1	5.4×10^5; 4.5×10^5
C57BL/6	High	2	3.9×10^5; 6.3×10^5
C57BL/6	High	3	6.3×10^5; 7.8×10^5
C57BL/6	High	4	3.3×10^6; 4.5×10^6
C57BL/6	High	8	5.1×10^6; 3.9×10^6
C57BL/6	High	12	8.0×10^4; 1.0×10^5
C57BL/6	High	15	7.5×10^4; 9.0×10^4
C57BL/6	High	25	ND; ND
BALB/c	Low	7	1.0×10^4; 1.0×10^4
BALB/c	High	7	5.1×10^6; 7.8×10^6
BALB/c-IFN-$\gamma^{-/-}$	High	7	7.2×10^6; 9.3×10^6

[a] Titers are given in PFU LCMV-WE per liver; ND, LCMV titers were below the detection limit of the plaque assay.

constitutive proteasome subunits δ and MB1 had not yet reached preinfection levels.

To investigate how mRNA levels of inducible and constitutive subunits were changed during the infection, we analyzed two C57BL/6 mice on days 0, 4, 8, and 11 of infection by real-time RT-PCR using the mRNA level of HPRT as a standard. As shown in Table II, the mRNAs for LMP2 and LMP7 were elevated by factors of 3.95 and 2.55 on day 8 of infection, respectively, and declined thereafter, which correlated with the incorporation of the respective proteins into proteasomes. Much less expected was the well-reproducible decline in the mRNAs for the constitutive subunits δ and MB1, which we have not observed in previous studies when cells were treated with IFN-γ in vitro (54). The factors responsible for this mRNA down-regulation of δ and MB1 in vivo remain to be identified. To examine whether IFN-γ and TNF-α, which have been shown to enhance LMP2 and LMP7 in vitro, are actually elevated during the infection we quantified their mRNA from the same cDNA samples. The elevations of IFN-γ and TNF-α mRNAs on day 4 of infection were only 1.61- and 3.2-fold, respectively, thus raising some doubt as to whether such a weak up-regulation can be sufficient to transcriptionally induce LMP2 and LMP7 or whether other cytokines are involved at that stage. On day 8 of infection, however, the 5.5-fold elevation of IFN-γ and the 43.0-fold elevation of TNF-α are consistent with these cytokines being responsible for immunosubunit induction at the peak of the CTL response. The results were also congruent with our histological examination, which revealed a massive infiltration of lymphocytes on day 8, but not yet on day 4, of LCMV infection (data not shown) in accordance with previous studies (47). Western analysis was performed to determine the expression levels of LMP2/δ and LMP7/MB1 in lysates of liver samples throughout the course of LCMV infection and fully confirmed the results obtained with two-dimensional gels (Fig. 2*C*). The synthesis of LMP7 precursors on day 8 of infection was apparently so strong that not all 30-kDa precursors could be incorporated into assembling proteasomes, as they were found on the top of sucrose gradients in contrast to the α-type subunit MC3 (Fig. 2*D*).

To investigate whether the in vivo replacement of proteasomes can also be observed in mice of a different MHC haplotype and genetic background, we infected BALB/c mice with a high dose of LCMV-WE and likewise isolated and analyzed 20S proteasomes of the liver. Also in the BALB/c strain we repeatedly observed a virtually complete exchange of constitutive proteasomes by immunoproteasomes already on day 7 postinfection (Fig. 3*A*). This phenomenon was not dependent on infections with high doses of LCMV-WE, as the subunit replacements were similar in the liver of BALB/c mice that had been infected for 7 days with a low dose of LCMV-WE (200 PFU), which is normally used as a physiological equivalent in this experimental system. The quantitative analysis of the two-dimensional gels from the high dose and low dose infections (Fig. 3*B*) confirmed that the virus dose did not alter the rate of proteasome subunit replacements, and the same result was obtained when C57BL/6 mice were infected with 200 PFU LCMV-WE (data not shown).

In vivo replacement of δ and MB1 by LMP2 and LMP7 is largely dependent on IFN-γ, but only to a minor extent on IFN-α and perforin

Since IFN-γ is the cytokine that transcriptionally induces LMP2, LMP7, and MECL-1 most vigorously (55), we decided to determine the extent of subunit replacement in the liver of IFN-γ-deficient BALB/c mice (34) that had been infected with a high or a low dose of LCMV-WE 7 days previously (Fig. 4). In the absence of IFN-γ the induction of LMP2 and LMP7 was reduced by about 50% despite an enhanced virus titer, indicating that a complete replacement of active site proteasome subunits, as in the wild-type BALB/c mouse, could not be obtained. Hence, other cytokines must be able to induce the 7-fold induction of LMP2 and LMP7 observed in IFN-$\gamma^{-/-}$ mice. We tested the effects of IFN-α and -β in IFN-α$R^{-/-}$ mice and found that the replacement of constitutive proteasomes by immunoproteasomes in the liver was only slightly reduced. Apparently, type I IFNs do not contribute much to the proteasome replacement in vivo, which is consistent with a lack of LMP2 and LMP7 up-regulation after LCMV infection in vitro that led to an induction of IFN-α/β (data not shown). Another gene-targeted mouse that we examined was the perforin$^{-/-}$ mouse, because we wanted to determine whether perforin-mediated destruction of LCMV-infected cells in the liver by CTLs or NK cells would be required to promote the removal of constitutive proteasomes and the replacement by immunoproteasomes during tissue regeneration. As shown in the *bottom panel* of Fig. 4, perforin

Table II. *Real time RT-PCR analysis of mRNA levels in the liver of C57BL/6 mice on different days of infection with 10^6 PFU of LCMV-WE*[a]

Day	LMP2	LMP7	δ	MB1	IFN-γ	TNF-α
0	1.0	1.0	1.0	1.0	1.0	1.0
4	2.61 ± 0.77	1.63 ± 0.08	0.81 ± 0.12	0.84 ± 0.12	1.61 ± 0.19	3.20 ± 1.27
8	3.95 ± 1.48	2.55 ± 0.35	0.62 ± 0.13	0.71 ± 0.12	5.50 ± 0.55	43.0 ± 15.4
11	2.79 ± 1.54	1.35 ± 0.21	0.40 ± 0.16	1.10 ± 0.14	2.55 ± 1.06	18.2 ± 2.05

[a] Values represent factors of mRNA expression relative to the expression on day 0. Data are the means ± SD from values of two mice. The mRNA expression for HPRT was used to standardize the amount of cDNA, and results were very similar when β-actin was used as a standard (data not shown).

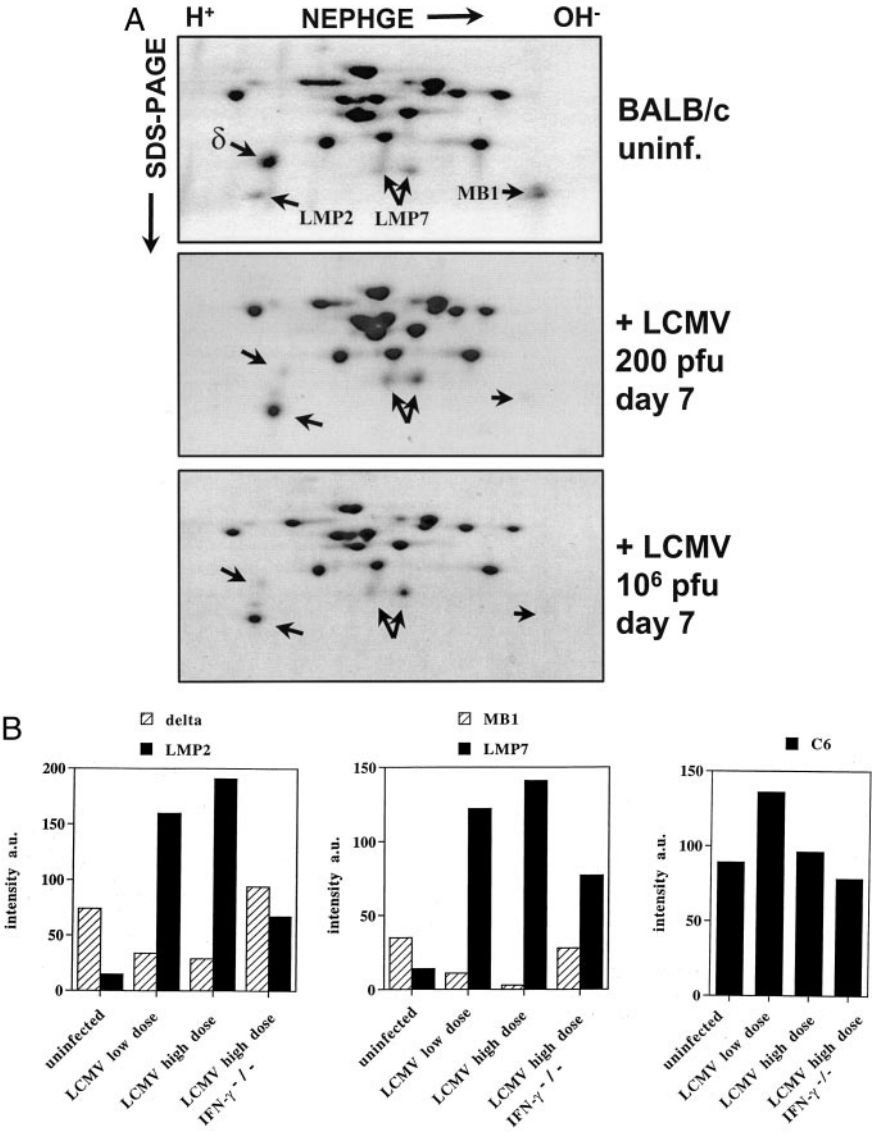

FIGURE 3. Composition of 20S proteasome subunits from livers of BALB/c mice after low dose and high dose infections with LCMV-WE. *A*, NEPHGE/SDS-PAGE analysis of 60 μg 20S proteasome purified from the liver of uninfected BALB/c mice or mice on day 7 after infection with high (10^6 PFU) or low (200 PFU) doses of LCMV-WE as indicated. The proteins were visualized by Coomassie stain, the positions of proteasome subunits LMP2, LMP7, Δ, and MB1 are marked. *B*, Densitometric evaluation of two-dimensional gels containing proteasome subunits from uninfected and infected BALB/c mice (*A*) and LCMV-infected IFN-$\gamma^{-/-}$ mice (Fig. 4).

deficiency affected the replacement of constitutive proteasomes in the liver to only a minor extent, suggesting that perforin-mediated cell death contributed only marginally to these replacements.

Infection of mice with Listeria *leads to an extensive replacement of constitutive proteasomes by immunoproteasomes in the liver*

We investigated whether the proteasome replacements in the liver during LCMV infection was a virus-specific phenomenon or whether an immune response against bacteria would have a similar consequence. BALB/c mice were infected i.v. with 9800 CFU of the Lm strain 10304S, and livers were removed on days 3 and 7 postinfection for isolation of 20S proteasomes and analysis on Coomassie-stained two-dimensional gels. As depicted in Fig. 5, Lm infection led to a comparable exchange of constitutive proteasomes by immunoproteasomes as had previously been observed with LCMV infection. The onset of proteasome replacements appeared to be very early after Lm infection, as it was more pronounced on day 3 of Lm infection than on day 4 after LCMV infection, a finding that was consistently obtained in both BALB/c (Fig. 5) and C57BL6 (data not shown) mice. Taken together, the extensive proteasome exchanges observed during the course of LCMV infection do not seem to be a solitary phenomenon confined to this virus, but may be extended to bacteria and possibly other pathogens.

PA28α and β are up-regulated, whereas PA28γ is down-regulated, in the liver of LCMV-infected mice

Since PA28α/β is known to be transcriptionally up-regulated by IFN-γ and since PA28γ was reported to be down-regulated by IFN-γ by a to date uncharacterized post-transcriptional mechanism, we decided to follow the protein levels of PA28-α, -β, and -γ by Western analysis using peptide antisera against these three subunits of proteasome regulators. Liver tissues were obtained from C57BL/6 mice that were either uninfected or infected with a high dose of LCMV-WE on the indicated days before analysis (Fig. 6). The Western blots revealed that the amounts of PA28α and -β increased by a factor of 3.5 from day 0 to day 8 of infection and declined thereafter. As we have observed for the induction of LMP2 and LMP7, the induction was already visible on day 3 after LCMV infection and reached a peak when the CTL response is expected to be maximal on day 8. Interestingly, the level of PA28γ protein was strongly reduced during days 4, 8, and 15 of infection compared with that in uninfected mice, which has not previously been documented for a viral infection. In contrast to the induction

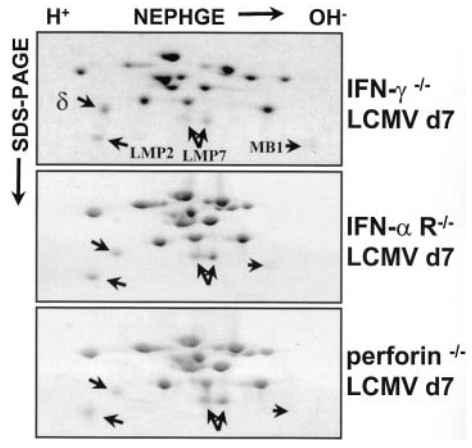

FIGURE 4. Liver proteasomes from LCMV-infected mice deficient for IFN-γ, IFN-αR, and perforin were analyzed. 20S proteasomes were purified from the livers of IFN-$\gamma^{-/-}$ (*top*), IFN-$\alpha R^{-/-}$ (*middle*), and perforin$^{-/-}$ (*bottom*) mice 7 days after infection with 10^6 PFU LCMV-WE. Proteasome subunits were separated on NEPHGE/SDS-PAGE and stained with Coomassie blue. The positions of proteasome subunits LMP2, LMP7, Δ, and MB1 are indicated.

of LMP2 and LMP7 that occurred at least to some degree in IFN-$\gamma^{-/-}$ mice, neither the induction of PA28α/β nor the disappearance of PA28γ occurred on day 7 after LCMV infection in the absence of IFN-γ, indicating that other cytokines cannot compensate for the lack of IFN-γ in this respect.

The peptidolytic activity of liver 20S proteasomes is strongly altered during the infection with LCMV

To address what consequences the proteasome subunit replacements during LCMV infection have on proteasome activity, we determined the activity of purified 20S proteasomes from livers of uninfected BALB/c mice as well as livers of LCMV-infected BALB/c wild type and IFN-$\gamma^{-/-}$ mice 7 days postinfection in peptidolytic assays. The respective 20S proteasomes, which were the same as those analyzed on the two-dimensional gels in Figs. 3 and 4, were incubated with the fluorogenic peptide substrates (Z)-LLE-β-nitroanilide (βNA), Suc-LLVY-7-amido-4-methylcoumarin (MCA), (Z)-GGL-MCA, and Bz-VGR-MCA, and the release of the fluorogenic leaving groups βNA or MCA was measured at different substrate concentrations after 30, 60, and 90 min. The 60-min values of the linear and very reproducible reaction are

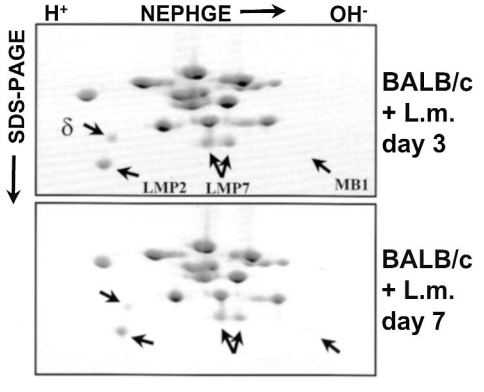

FIGURE 5. Effect of Lm infection on proteasome subunit composition in the mouse liver. BALB/c mice were infected with 9800 CFU Lm 10304S, and 20S proteasomes were purified from livers on days 3 and 7 after infection. Proteasome subunits were separated on NEPHGE/SDS-PAGE and stained with Coomassie blue.

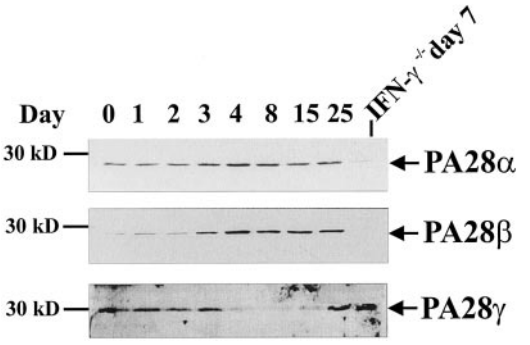

FIGURE 6. Western analysis of PA28-α, -β, and -γ expression in the livers of LCMV-infected mice. Liver samples were taken from C57BL/6 wild-type mice that were either uninfected (day 0) or had been infected with 10^6 PFU LCMV-WE on the indicated days before hepatectomy. For comparison, an IFN-$\gamma^{-/-}$ BALB/c mouse was analyzed on day 7 post-LCMV infection. Total lysates of liver samples were blotted and probed with antisera specific for PA28α, PA28β, and PA28γ as indicated, and reactive bands were visualized on x-ray films by ECL. The position of a 30-kDa marker is indicated on the *left*.

shown in Fig. 7 and indicate that the cleavage of the (Z)-LLE-βNA substrate at the C terminus of glutamic acid, which is frequently used to determine the peptidylglutamyl peptide-hydrolyzing or

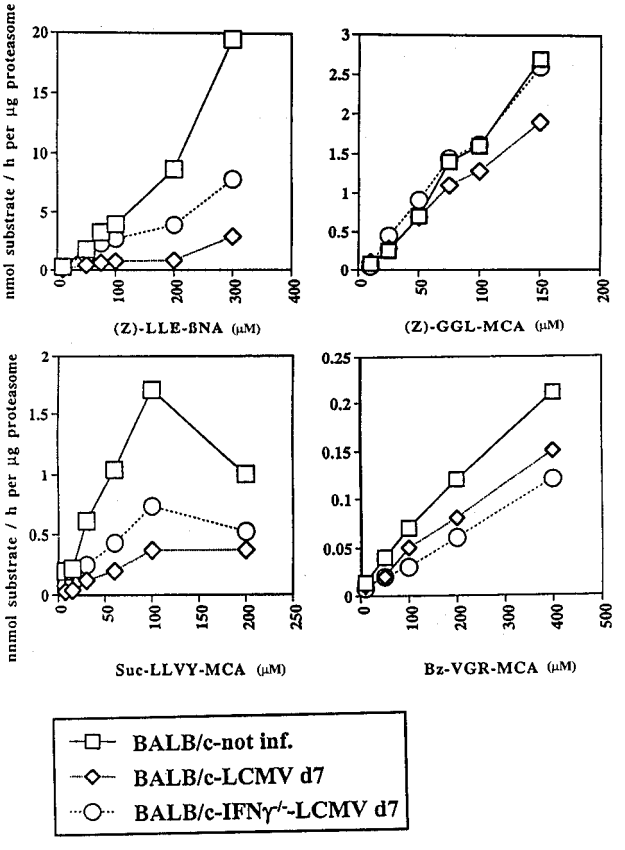

FIGURE 7. Peptide hydrolyzing activity of 20S proteasomes purified from the livers of LCMV-infected and uninfected (not inf.) BALB/c mice. The purified 20S proteasomes from livers of uninfected BALB/c mice or LCMV-WE-infected BALB/c wild-type and IFN-$\gamma^{-/-}$ mice (the same preparations as analyzed in Figs. 3 and 4) were assayed for hydrolysis of the indicated fluorogenic substrates at various concentrations. The activities are calculated from fluorescence of the MCA or βNA leaving groups after 60 min of incubation. Values are the means of triplicate determinations with an SE of <5% for all data points. d, Day.

caspase-like activity of the proteasome, was almost completely lost on day 7 of LCMV infection in wild-type mice and was reduced by approximately 50% in IFN-$\gamma^{-/-}$ mice. According to our previous transfection experiments (8, 10), this dramatic change in the caspase-like activity must be due to the replacement of δ by LMP2, which is almost quantitative in liver proteasomes on day 7 post-LCMV infection. The trypsin-like activity, as determined by hydrolysis of the Bz-VGR-MCA substrate, was slightly reduced in LCMV-infected mice, whereas the chymotrypsin-like activity measured by hydrolysis of (Z)-GGL-MCA was not significantly different among the three proteasome populations. The hydrolysis of the Suc-LLVY-MCA substrate, in contrast, was markedly reduced in liver proteasomes of LCMV-infected mice, as we had observed consistently in cell lines after IFN-γ treatment and in cell lines transfected with LMP2, LMP7, and MECL-1 (7, 8, 10). Together, the results obtained corresponded very well with data obtained in LMP2/LMP7/MECL-1 triple transfectants (56), indicating that these marked changes in proteasome activity are probably attributed to the almost complete replacement of constitutive proteasomes by immunoproteasomes in the liver of LCMV-infected mice.

Discussion

In this study we analyzed to what extent an exchange of constitutive proteasomes by immunoproteasomes occurs at the steady state level during viral or bacterial infection of an animal. We found that the replacement of constitutive proteasomes by immunoproteasomes in the liver starts on day 2 of LCMV or Lm infection and gradually proceeds to an almost complete exchange of proteasomes in this organ by day 7 or 8 of infection. Simultaneously, the expression of PA28α/β is markedly enhanced, while the PA28γ regulator disappears. The extent of 20S proteasome replacement in the liver is striking and indicates that immunoproteasomes can take over the numerous housekeeping functions of constitutively expressed proteasomes at least for a few days. In the priming phase of the cytotoxic immune response 4 days after LCMV infection, the proteasome population in the liver consists of about equal amounts of immunoproteasomes and constitutive proteasomes, which may enhance the diversity of Ag processing. In the main effector phase of the CTL response on day 7 or 8 after infection, however, the balance is shifted toward immunoproteasomes, suggesting that the recognition of infected cells and the clearance of the pathogen rely on the presentation of epitopes that are produced by immunoproteasomes under an increased influence of the PA28α/β regulator.

The short time period of 7 days in vivo until the constitutive proteasomes containing the active site subunits δ and MB1 disappear is unexpected, since 20S proteasomes were shown to have an extraordinarily long half-life of 12–15 days in the liver of metabolically labeled rats (53). Since the replacement of active site subunits in the proteasome population cannot occur in preformed and matured 20S proteasomes (55), it relies on the de novo assembly of immunoproteasomes and the relative loss of constitutive proteasomes. Because of the long half-life of 20S proteasomes, we expected that immunoproteasomes would at best add a population to the pre-exisiting constitutive pool until the virus is cleared. A possible explanation for the rapid elimination of housekeeping proteasomes in the inflamed liver would be a massive destruction of LCMV-infected hepatocytes by virus-specific CTLs. Indeed, serum levels of liver enzymes such as alanine aminotransferase or aspartate aminotransferase were shown to transiently rise by a factor of 10–20 in LCMV-WE-infected mice, indicating the lysis of hepatocytes (47). However, based on the enhancement of alanine aminotransferase levels, it has been estimated that only 5% of hepatocytes are lysed during an acute immune response to LCMV-WE (49) in accordance with the small effect that perforin deficiency had on proteasome replacements in the liver (Fig. 4). A histological assessment of LCMV infection by in situ hybridization indicated that only 5–10% of hepatocytes contained the viral mRNA on day 5 after infection, whereas all Kupffer cells were infected (49). Even if the destroyed tissue would be immediately replaced by new hepatocytes, a cellular turnover of 10% within 7 days would not suffice to account for a complete proteasome exchange if the half-life of constitutive proteasomes in the liver is 12–15 days. It will therefore be interesting to determine the in vivo half-life of constitutive proteasomes in the liver of LCMV-infected and uninfected mice to test whether an accelerated degradation of constitutive 20S proteasomes may occur in inflamed organs. An alternative contribution to the change in proteasome composition could be the infiltration of the liver with leukocytes that possess roughly equal amounts of immunoproteasomes and constitutive proteasomes in the uninduced state. The total lymphocyte number in the liver increases by a factor of 100 from day 4 until day 6, adding up to a total of 20 million lymphocytes/liver throughout days 6–10 of infection (47). However, even in the peak phase of the immune response the cell number of lymphocytes is about 10-fold lower than the number of the much larger hepatocytes and hence contributes only marginally to the total proteasome pool of the liver.

Our experiments performed in IFN-γ-deficient mice showed that the induction of PA28α/β as well as the disappearance of PA28γ relied entirely on IFN-γ production in the LCMV-infected liver. While a vigorous induction of PA28α/β by IFN-γ could be predicted from previous in vitro data (25), the disappearance of PA28γ after IFN-γ treatment has not been observed in all cell lines (M. Groettrup, unpublished observations) and is still a matter of debate. Our in vivo data clearly support this phenomenon first observed by Tanahashi et al. (32) and pose the question of its functional implication. One could imagine that PA28γ competes with PA28α/β for binding to the proteasome, which may adversely affect Ag processing, and we are currently addressing this possibility in our laboratory. Also, the mechanism that leads to the down-regulation of PA28γ protein during LCMV infection needs to be investigated, because mRNA levels of PA28γ are not affected by IFN-γ treatment of cells in vitro (25). In contrast to the alteration of PA28 regulators, the replacement of δ, MB1, and MC14 by LMP2, LMP7, and MECL-1 did occur in IFN-γ-deficient mice, albeit at a 50% reduced level. Thus, IFN-γ is required for a full replacement of constitutive proteasomes by immunoproteasomes, but other factors must be able to cause a half-maximal exchange. TNF-α is a prime candidate to mediate this effect, as it is known to induce LMP2 and LMP7 in vitro (55), and since TNF-α mRNA has been found in the liver 2 days after LCMV-WE infection (49). The cells that produce IFN-γ and TNF-α during the first 4 days of infection are most likely NK cells, NKT cells, and macrophages, respectively. NK cells are found in 4-fold greater number between days 1–5 of LCMV infection in the liver (57). However, our real-time RT-PCR analysis revealed that the enhancement of TNF-α and IFN-γ mRNAs was not very prominent in the liver of C57BL/6 mice on day 4 after LCMV-WE infection (Table II), which could indicate that other cytokines may also contribute to the early induction of immunoproteasomes. Beginning on day 5 of infection, LCMV-specific CTLs and Th cells can be found in the liver (data not shown) (47), which are likely to account for the strongly elevated levels of IFN-γ and TNF-α observed on day 8 of infection.

Another class of cytokines that is immediately induced after LCMV infection in vivo is IFN-α/β (58, 59). LCMV is a (−) strand RNA virus that replicates via dsRNA intermediates known

to be potent inducers of IFN-α/β. Nevertheless, we could not observe an induction of PA28α (data not shown) or LMP2 and LMP7 after productive infection of a fibroblast line, although the induction of IFN-β could be demonstrated by RT-PCR after LCMV-WE infection in vitro (K. Schwarz, unpublished observations). This indicates that a cell-autonomous production of IFN-α/β does not effectively induce immunoproteasomes and that other cytokines, such as IFN-γ and TNF-α, are required. In accordance with this result, a deficiency of the IFN-αR only marginally affected proteasome exchange in mouse liver after LCMV infection (Fig. 4).

What consequences does virtually complete replacement of constitutive proteasomes by immunoproteasomes have on our understanding of the immune response to LCMV in particular and of the functions of LMP2, LMP7, and MECL-1 induction in general? Although the CTL response against LCMV has not yet been investigated in mice that are deficient for LMP2 or LMP7, it is already clear from studies in IFN-γR$^{-/-}$ mice that the IFN-γ-mediated induction of these proteasome components is not required for elimination of the virus, although virus titers were elevated and the CTL response reduced when the IFN-γR was genetically ablated (35) or when IFN-γ was neutralized by Abs in vivo (60, 61). With respect to the generation of LCMV epitopes, we have recently shown that the transfection of fibroblasts with LMP2, LMP7, and MECL-1 results in a markedly enhanced presentation of the H-2L^d-restricted nucleoprotein epitope nucleoprotein 118 and that purified immunoproteasomes produced 6-fold more precursors of this epitope compared with constitutive proteasomes in vitro (22). Recently, we have investigated the generation of the H-2D^b-restricted glycoprotein epitopes GP33 and GP276 and found that IFN-γ treatment of fibroblasts led to a 4-fold enhanced presentation of the immunodominant GP33 epitope, whereas the subdominant GP276 was 3-fold down-regulated (K. Schwarz, unpublished observations), and we are currently investigating whether these changes can be attributed to alterations in proteasome composition.

If immunoproteasomes are not required for the bulk production of MHC class I ligands and if some epitopes are dependent on LMP2, LMP7, and MECL-1, while others, including important tumor epitopes, are destroyed, why, then, would an inducible expression of immuoproteasomes occur in sites of viral infection? The surprising finding of an almost complete replacement of constitutive proteasomes by immunoproteasomes suggests that rather than increasing the diversity of proteasome populations, immunoproteasomes serve to generate different T cell epitopes in inflamed as opposed to uninflamed tissues, which normally express extremely low levels of LMP2, LMP7, and MECL-1 (54). We hypothesize that the replacement of proteasomes in inflamed tissues serves to focus the immune response on T cell epitopes that are preferentially or exclusively made by immunoproteasomes. This change in epitope production may also contribute to avoid autoimmune assaults if different peptide epitopes are processed from endogenous housekeeping genes in uninflamed sites as opposed to sites of viral infection. T cells that recognize an immunoproteasome or PA28α/β - dependent peptide from a household protein in an inflammatory site may not find the same peptide in uninflamed tissues and hence would not cause tissue damage in inappropriate sites.

Acknowledgments

We thank Rolf M. Zinkernagel and Gunter Schmidtke for critical reading of the manuscript and for technical advice. Manfred Kopf is acknowledged for providing the IFN-γ-deficient mice, and Peter-M. Kloetzel, Ulrike Kuckelkorn, Alice Sijts, and Klavs Hendil for contributing Abs. We are grateful to Nathalie Oetiker and Hans Christian Probst for help with LCMV infection of mice.

References

1. Voges, D., P. Zwickl, and W. Baumeister. 1999. The 26S proteasome: a molecular machine designed for controlled proteolysis. *Annu. Rev. Biochem. 68:1015.*
2. Groettrup, M., A. Soza, U. Kuckelkorn, and P. M. Kloetzel. 1996. Peptide antigen production by the proteasome: complexity provides efficiency. *Immunol. Today 17:429.*
3. Gaczynska, M., K. L. Rock, and A. L. Goldberg. 1993. γ-Interferon and expression of MHC genes regulate peptide hydrolysis by proteasomes. *Nature 365:264.*
4. Driscoll, J., M. G. Brown, D. Finley, and J. J. Monaco. 1993. MHC-linked LMP gene products specifically alter peptidase activities of the proteasome. *Nature 365:262.*
5. Eleuteri, A. M., R. A. Kohanski, C. Cardozo, and M. Orlowski. 1997. Bovine spleen multicatalytic proteinase complex (proteasome): replacement of X, Y, and Z subunits by LMP7, LMP2, and MECL1 and changes in properties and specificity. *J. Biol. Chem. 272:11824.*
6. Ustrell, V., G. Pratt, and M. Rechsteiner. 1995. Effects of interferon γ and major histocompatibility complex-encoded subunits on peptidase activities of human multicatalytic proteases. *Proc. Natl. Acad. Sci. USA 92:584.*
7. Boes, B., H. Hengel, T. Ruppert, G. Multhaup, U. H. Koszinowski, and P. M. Kloetzel. 1994. Interferon γ stimulation modulates the proteolytic activity and cleavage site preference of 20S mouse proteasomes. *J. Exp. Med. 179:901.*
8. Groettrup, M., T. Ruppert, L. Kuehn, M. Seeger, S. Standera, U. Koszinowski, and P. M. Kloetzel. 1995. The interferon-γ-inducible 11S regulator (PA28) and the LMP2/LMP7 subunits govern the peptide production by the 20S proteasome in vitro. *J. Biol. Chem. 270:23808.*
9. Gaczynska, M., K. L. Rock, T. Spies, and A. L. Goldberg. 1994. Peptidase activities of proteasomes are differentially regulated by the major histocompatibility complex-encoded genes for LMP 2 and LMP 7. *Proc. Natl. Acad. Sci. USA 91:9213.*
10. Kuckelkorn, U., S. Frentzel, R. Kraft, S. Kostka, M. Groettrup, and P.-M. Kloetzel. 1995. Incorporation of major histocompatibility complex-encoded subunits LMP2 and LMP7 changes the quality of the 20S proteasome polypeptide processing products independent of interferon-γ. *Eur. J. Immunol. 25:2605.*
11. Salzmann, U., S. Kral, B. Braun, S. Standera, M. Schmidt, P. M. Kloetzel, and A. Sijts. 1999. Mutational analysis of subunit iβ2 (MECL-1) demonstrates conservation of cleavage specificity between yeast and mammalian proteasomes. *FEBS Lett 454:11.*
12. Groll, M., L. Ditzel, J. Löwe, D. Stock, M. Bochtler, H. D. Bartunik, and R. Huber. 1997. Structure of 20 S proteasome from yeast at 2.4A resolution. *Nature 386:463.*
13. Arnold, D., J. Driscoll, M. Androlewicz, E. Hughes, P. Cresswell, and T. Spies. 1993. Proteasome subunits encoded in the MHC are not generally required for the processing of peptides bound by MHC class I molecules. *Nature 360:171.*
14. Momburg, F., V. Ortiz-Navarrete, J. Neefjes, E. Goulmy, Y. van-de-Wal, H. Spits, S. J. Powis, G. W. Butcher, J. C. Howard, P. Walden, and G. Haemmerling. 1993. Proteasome subunits encoded by the major histocompatibility complex are not essential for antigen presentation. *Nature 360:174.*
15. Van Kaer, L., P. G. Ashton-Rickardt, M. Eichelberger, M. Gaczynska, K. Nagashima, K. L. Rock, A. L. Goldberg, P. C. Doherty, and S. Tonegawa. 1994. Altered peptidase and viral-specific T cell response in LMP 2 mutant mice. *Immunity 1:533.*
16. Sibille, C., K. G. Gould, K. Willard-Gallo, S. Thomson, A. J. Rivett, S. Powis, G. W. Butcher, and P. De Baetselier. 1995. LMP2$^+$ proteasomes are required for the presentation of specific antigens to cytotoxic T lymphocytes. *Curr. Biol. 5:923.*
17. Fehling, H. J., W. Swat, C. Laplace, R. Kuehn, K. Rajewsky, U. Mueller, and H. von Boehmer. 1994. MHC class I expression in mice lacking proteasome subunit LMP-7. *Science 265:1234.*
18. Gileadi, U., H. T. MoinsTeisserenc, I. Correa, B. L. Booth, P. R. Dunbar, A. K. Sewell, J. Trowsdale, R. E. Phillips, and V. Cerundolo. 1999. Generation of an immunodominant CTL epitope is affected by proteasome subunit composition and stability of the antigenic protein. *J. Immunol. 163:6045.*
19. Sewell, A. K., D. A. Price, H. Teisserenc, B. L. Booth, U. Gileadi, F. M. Flavin, J. Trowsdale, R. E. Phillips, and V. Cerundolo. 1999. IFN-γ exposes a cryptic cytotoxic T lymphocyte epitope in HIV-1 reverse transcriptase. *J. Immunol. 162: 7075.*
20. Sijts, A. J. A. M., S. Standera, R. E. M. Toes, T. Ruppert, N. J. C. M. Beekman, P. A. van Veelen, F. A. Ossendorp, C. J. M. Melief, and P. M. Kloetzel. 2000. MHC class I antigen processing of an adenovirus CTL epitope is linked to the levels of immunoproteasomes in infected cells. *J. Immunol. 164:4500.*
21. Sijts, A. J. A. M., T. Ruppert, B. Rehermann, M. Schmidt, U. Koszinowski, and P. M. Kloetzel. 2000. Efficient generation of a hepatitis B virus cytotoxic T lymphocyte epitope requires the structural features of immunoproteasomes. *J. Exp. Med. 191:503.*
22. Schwarz, K., M. van den Broek, S. Kostka, R. Kraft, A. Soza, G. Schmidtke, P. M. Kloetzel, and M. Groettrup. 2000. Overexpression of the proteasome subunits LMP2, LMP7, and MECL-1 but not PA28α/β enhances the presentation of an immunodominant lymphocytic choriomeningitis virus T cell epitope. *J. Immunol. 165:768.*
23. Morel, S., F. Levy, O. BurletSchiltz, F. Brasseur, M. ProbstKepper, A. L. Peitrequin, B. Monsarrat, R. VanVelthoven, J. C. Cerottini, T. Boon, et al. 2000. Processing of some antigens by the standard proteasome but not by the

immunoproteasome results in poor presentation by dendritic cells. *Immunity 12: 107.*

24. Chen, W. S., C. C. Norbury, Y. J. Cho, J. W. Yewdell, and J. R. Bennink. 2001. Immunoproteasomes shape immunodominance hierarchies of antiviral CD8(+) T cells at the levels of T cell repertoire and presentation of viral antigens. *J. Exp. Med. 193:1319.*
25. Ahn, J. Y., N. Tanahashi, K.-y. Akiyama, H. Hisamatsu, C. Noda, K. Tanaka, C. H. Chung, N. Shibmara, P. J. Willy, J. D. Mott, et al. 1995. Primary structures of two homologous subunits of PA28, a γ-interferon-inducible protein activator of the 20S proteasome. *FEBS Lett. 366:37.*
26. Dick, T. P., T. Ruppert, M. Groettrup, P. M. Kloetzel, L. Kuehn, U. H. Koszinowski, S. Stevanovic′, H. Schild, and H.-G. Rammensee. 1996. Coordinated dual cleavages by the proteasome regulator PA28 lead to dominant MHC ligands. *Cell 86:253.*
27. Niedermann, G., R. Grimm, E. Geier, M. Maurer, C. Realini, C. Gartmann, J. Soll, S. Omura, M. C. Rechsteiner, W. Baumeister, et al. 1997. Potential immunocompetence of proteolytic fragments produced by proteasomes before evolution of the vertebrate immune system. *J. Exp. Med. 186:209.*
28. Groettrup, M., A. Soza, M. Eggers, L. Kuehn, T. P. Dick, H. Schild, H.-G. Rammensee, U. H. Koszinowski, and P.-M. Kloetzel. 1996. A role for the proteasome regulator PA28α in antigen presentation. *Nature 381:166.*
29. van Hall, T., A. Sijts, M. Camps, R. Offringa, C. Melief, P. M. Kloetzel, and F. Ossendorp. 2000. Differential influence on cytotoxic T lymphocyte epitope presentation by controlled expression of either proteasome immunosubunits or PA28. *J. Exp. Med. 192:483.*
30. Schwarz, K., M. Eggers, A. Soza, U. H. Koszinowski, P. M. Kloetzel, and M. Groettrup. 2000. The proteasome regulator PA28α/β can enhance antigen presentation without affecting 20S proteasome subunit composition. *Eur. J. Immunol. 30:3672.*
31. Preckel, T., W. Fung-Leung, Z. Cai, A. Vitiello, L. Salter-Cid, O. Winqvist, T. G. Wolfe, M. von Herrath, A. Angulo, P. Ghazal, et al. 1999. Impaired immunoproteasome assembly and immune responses in PA28$^{-/-}$ mice. *Science 286:2162.*
32. Tanahashi, N., K.-y. Yokota, J. Y. Ahn, C. H. Chung, T. Fijiwara, E.-i. Takahashi, G. N. DeMartino, C. A. Slaughter, T. Toyonaga, K.-i. Yamamura, et al. 1997. Molecular properties of the proteasome activator PA28 family proteins and γ-interferon regulation. *Genes Cells 2:195.*
33. Murata, S., H. Kawahara, S. Tohma, K. Yamamoto, M. Kasahara, Y. Nabeshima, K. Tanaka, and T. Chiba. 1999. Growth retardation in mice lacking the proteasome activator PA28γ. *J. Biol. Chem. 274:38211.*
34. Dalton, D. K., S. Pitts-Meek, S. Keshav, I. S. Figari, A. Bradley, and T. A. Stewart. 1993. Multiple defects of immune cell function in mice with disrupted interferon-γ genes. *Science 259:1739.*
35. Müller, U., U. Steinhoff, L. F. Reis, S. Hemmi, J. Pavlovic, R. M. Zinkernagel, and M. Aguet. 1994. Functional role of type I and type II interferons in antiviral defense. *Science 264:1918.*
36. Kägi, D., B. Ledermann, K. Burki, P. Seiler, B. Odermatt, K. J. Olsen, E. R. Podack, R. M. Zinkernagel, and H. Hengartner. 1994. Cytotoxicity mediated by T cells and natural killer cells is greatly impaired in perforin-deficient mice. *Nature 369:31.*
37. Aden, D. P., and B. B. Knowles. 1976. Cell surface antigens coded for by the human chromosome 7. *Immunogenetics 3:209.*
38. Schwarz, K., R. de Giuli, G. Schmidtke, S. Kostka, M. van den Broek, K. Kim, C. M. Crews, R. Kraft, and M. Groettrup. 2000. The selective proteasome inhibitors lactacystin and expoxomicin can be used to either up- or downregulate antigen presentation at non-toxic doses. *J. Immunol. 164:6147.*
39. Bruns, M., J. Cihak, G. Müller, and F. Lehmann-Grube. 1983. Lymphocytic choriomeningitis virus. VI. Isolation of a glycoprotein mediating neutralization. *Virology 130:247.*
40. Lehmann-Grube, F. 1971. Lymphocytic choriomeningitis virus. *Virol. Monogr. 10:1.*
41. Battegay, M., S. Cooper, A. Althage, J. Banziger, H. Hengartner, and R. M. Zinkernagel. 1991. Quantification of lymphocytic choriomeningitis virus with an immunological focus assay in 24- or 96-well plates. *J. Virol. Methods 33:191.*
42. Schmidtke, G., S. Emch, M. Groettrup, and H. G. Holzhütter. 2000. Evidence for the existence of a non-catalytic modifier site of peptide hydrolysis by the 20S proteasome. *J. Biol. Chem. 275:22056.*
43. Schmidtke, G., H. Holzhütter, M. Bogyo, N. Kairies, M. Groll, R. de Giuli, S. Emch, and M. Groettrup. 1999. How an inhibitor of the HIV-1 protease modulates proteasome activity. *J. Biol. Chem. 274:35734.*
44. Groettrup, M., R. Kraft, S. Kostka, S. Standera, R. Stohwasser, and P.-M. Kloetzel. 1996. A third interferon-γ-induced subunit exchange in the 20S proteasome. *Eur. J. Immunol. 26:863.*
45. Macagno, A., M. Gilliet, F. Sallusto, A. Lanzavecchia, F. O. Nestle, and M. Groettrup. 1999. Dendritic cells upregulate immunoproteasomes and the proteasome regulator PA28 during maturation. *Eur. J. Immunol. 29:4037.*
46. Seelig, A., B. Boes, and P. M. Kloetzel. 1993. Characterization of mouse proteasome subunit MC3 and identification of proteasome subtypes with different cleavage characteristics. *Enzyme Protein 47:330.*
47. Zinkernagel, R., E. Haenseler, T. Leist, A. Cerny, H. Hengartner, and A. Althage. 1986. T cell-mediated hepatitis in mice infected with lymphocytic choriomeningitis virus. *J. Exp. Med. 164:1075.*
48. Guidotti, L. G., P. Borrow, A. Brown, H. McClary, R. Koch, and F. V. Chisari. 1999. Noncytopathic clearance of lymphocytic choriomeningitis virus from the hepatocyte. *J. Exp. Med. 189:1555.*
49. Guidotti, L. G., P. Borrow, M. V. Hobbs, B. Matzke, I. Gresser, M. B. A. Oldstone, and F. V. Chisari. 1996. Viral cross talk: intracellular inactivation of the hepatitis B virus during an unrelated viral infection of the liver. *Proc. Natl. Acad. Sci. USA 93:4589.*
50. Rotem-Yehudar, R., M. Groettrup, A. Soza, P. M. Kloetzel, and R. Ehrlich. 1996. LMP-associated proteolytic activities and TAP-dependent transport for class I MHC molecules are suppressed in cell lines transformed by the highly oncogenic adenovirus 12. *J. Exp. Med. 183:499.*
51. Zeidler, R., G. Eissner, P. Meissner, A. Uebel, R. Tampé, S. Lazis, and W. Hammerschmidt. 1997. Downregulation of TAP1 in B lymphocytes by cellular and Epstein-Barr virus-encoded interleukin-10. *Blood 6:2390.*
52. Moskophidis, D., F. Lechner, H. Pircher, and R. M. Zinkernagel. 1993. Virus persistence in acutely infected immunocompetent mice by exhaustion of antiviral cytotoxic effector T cells. *Nature 362:758.*
53. Tanaka, K., and A. Ichihara. 1989. Half-life of proteasomes (multiprotease complexes) in rat liver. *Biochem. Biophys. Res. Commun. 159:1309.*
54. Stohwasser, R., S. Standera, I. Peters, P.-M. Kloetzel, and M. Groettrup. 1997. Molecular cloning of the mouse proteasome subunits MC14 and MECL-1: reciprocally regulated tissue expression of interferon-γ-modulated proteasome subunits. *Eur. J. Immunol. 27:1182.*
55. Aki, M., N. Shimbara, M. Takashina, K. Akiyama, S. Kagawa, T. Tamura, N. Tanahashi, T. Yoshimura, K. Tanaka, and A. Ichihara. 1994. Interferon-γ induces different subunit organizations and functional diversity of proteasomes. *J. Biochem. 115:257.*
56. Groettrup, M., S. Standera, R. Stohwasser, and P. M. Kloetzel. 1997. The subunits MECL-1 and LMP2 are mutually required for incorporation into the 20S proteasome. *Proc. Natl. Acad. Sci. USA 94:8970.*
57. McIntyre, K. W., and R. M. Welsh. 1986. Accumulation of natural killer and cytotoxic T large granular lymphocytes in the liver during virus infection. *J. Exp. Med. 164:1667.*
58. Leist, T. P., M. Aguet, M. Hassig, D. C. Pevear, C. J. Pfau, and R. M. Zinkernagel. 1987. Lack of correlation between serum titers of interferon α, β, natural killer cell activity and clinical susceptibility in mice infected with two isolates of lymphocytic choriomeningitis virus. *J. Gen. Virol. 68:2213.*
59. Cousens, L. P., J. S. Orange, H. C. Su, and C. A. Biron. 1997. Interferon-α/β inhibition of interleukin 12 and interferon-γ production in vitro and endogenously during viral infection. *Proc. Natl. Acad. Sci. USA 94:634.*
60. Wille, A., A. Gessner, H. Lother, and F. Lehmann-Grube. 1989. Mechanism of recovery from acute virus infection. VIII. Treatment of lymphocytic choriomeningitis virus-infected mice with anti-interferon-γ monoclonal antibody blocks generation of virus-specific cytotoxic T lymphocytes and virus elimination. *Eur. J. Immunol. 19:1283.*
61. Leist, T. P., M. Eppler, and R. M. Zinkernagel. 1989. Enhanced virus replication and inhibition of lymphocytic choriomeningitis virus disease in anti-γ interferon-treated mice. *J. Virol. 63:2813.*